JOC The Journal of Organic Chemistry

Article

pubs.acs.org/joc

Photoremoval of Protecting Groups: Mechanistic Aspects of 1,3-Dithiane Conversion to a Carbonyl Group

Gabriela Oksdath-Mansilla,[†] Viviane Hajj,[‡] Diego M. Andrada,[§] Juan E. Argüello,[†] Julien Bonin,[‡] Marc Robert,*[,‡] and Alicia B. Peñéñory*[,†]

[†]INFIQC−CONICET-UNC, Departmento de Química Orgánica, Facultad de Ciencias Químicas, Universidad Nacional de Córdoba, Ciudad Universitaria, X5000HUA Córdoba, Argentina

[‡]Laboratoire d'Electrochimie Moléculaire, Unité Mixte de Recherche Université - CNRS No 7591, Université Paris Diderot, Sorbonne Paris Cité, Bâtiment Lavoisier, 15 rue Jean Antoine de Baïf, 75205 Paris Cedex 13, France

[§]Fachbereich Chemie, Philipps-Universität Marburg, Hans-Meerwein-Strasse, D-35032 Marburg, Germany

Supporting Information

ABSTRACT: Photodeprotection of 1,3-dithianes in the presence of thiapyrylium was performed to return to the parent carbonyl compound, and the mechanism was studied by steady state photolysis, laser flash photolysis, and theoretical calculations. Electron transfer from dithianes to triplet sensitizers is extremely fast, and the decay of dithiane radical cations was not affected by the presence of water or oxygen as the consequence of a favorable unimolecular fragmentation pathway. Similar behaviors were observed for dithianes bearing electron-releasing or electron-withdrawing substituents on the aryl moiety, evidenced by C−S bond cleavage to form a distonic radical cation species. The lack of reaction under nitrogen atmosphere, requirement of oxygen for good conversion yields, inhibition of the photodeprotection process by the presence of *p*-benzoquinone, and absence of a labeled carbonyl final product when the reaction is performed in the presence of $H_2{}^{18}O$ all suggest that the superoxide anion drives the deprotection reaction. Density functional theory computational studies on the reactions with water, molecular oxygen, and the superoxide radical anion support the experimental findings.

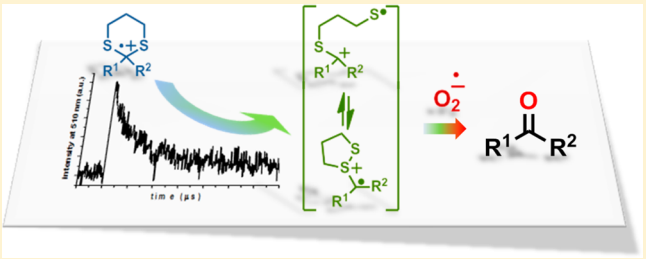

INTRODUCTION

Protection of carbonyl groups is often a necessary step in organic synthesis, especially in the total synthesis of natural products and multifunctional organic compounds. Thioacetals and cyclic thioacetals, such as 1,3-dithianes and 1,3-dithiolanes, are commonly used protecting groups due to their easy access and high stability under both acidic and basic conditions.[1]

Many procedures are available for thioacetal deprotection. They usually require drastic conditions, such as a stoichiometric or excess amount of toxic reactants, including Hg(II) and other heavy metal salts.[2] The later process has recently been used for sensitive and selective detection of Hg(II) and Cd(II).[3] Furthermore, there are methods that utilize heterogeneous conditions, using a variety of Fe(III)[4] and Cu(II)[5] salts, and other solvent-free methodologies have recently been reported.[6] The deprotection of 1,3-dithianes and 1,3-dithiolanes has also been performed under irradiation in the presence of a variety of sensitizers, including 2,4,6-triphenylpyrylium salts, chloranil (CA), dicyanoanthracene (DCA), methylene blue (MB), and methylene green (MG) under mild conditions.[7]

Because of their low oxidation potential, cyclic thioethers promptly undergo single-electron transfer (SET) oxidation. Thus, the participation of radical cation intermediates has been proposed for the oxidative cleavage of thioacetal.[7] However, the operating mechanism as well as the source of oxygen in these reactions are a matter of controversy (Scheme 1).[7,8] The mechanism proposed for the deprotection of dithianes **1** using either an indirect electrochemical oxidation procedure with tris(*p*-tolyl)amine as the homogeneous electron donor[9] or SET oxidants, such as $SbCl_5$,[8] $Cu(NO_3)_2$ 2.5H_2O/K-10,[6b] MG,[7d] or $Fe(phen)_3(PF_6)_3$ complexes,[10] involves the participation of a

Scheme 1. General Mechanism for the Electron Transfer Deprotection of Dithiane

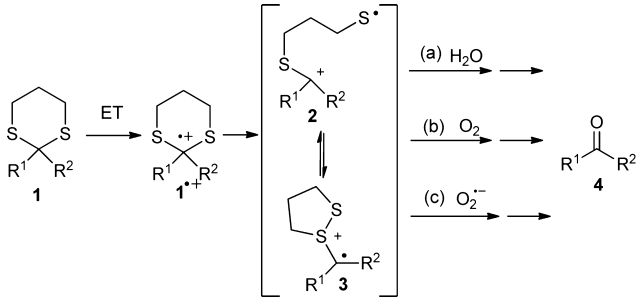

Received: December 31, 2014
Published: February 16, 2015

DOI: 10.1021/jo502953t
J. Org. Chem. 2015, 80, 2733−2739

radical cation $1^{\bullet+}$, which fragments into a distonic radical cation. The one-electron oxidation of the later species to a sulfonium ion is the key step for dethioacetalization, which possibly involves H_2O as a nucleophile (Scheme 1, pathway a).[8,10] In addition, during the photochemical dethioacetalization by 2,4,6-triphenylpyrylium tetrafluoroborate (TPPT) or methylacridinium perchlorate (MAP), fragmentation of $1^{\bullet+}$ into a distonic radical cation has been proposed to account for the formation of the carbonyl compound after a subsequent reaction with O_2 at the radical carbon center (Scheme 1, pathway b).[7e] Participation of the superoxide anion has also been proposed when using dicyanamide (DCA) (Scheme 1, pathway c).[7e] DCA indeed possesses a more negative reduction potential than O_2, and therefore the superoxide radical anion is in this case formed by a secondary electron transfer (ET) from the sensitizer radical anion.

On the other hand, for reactions in the presence of *meso*-tetraphenylporphine (TPP) and MB, the generation of singlet oxygen has been proposed to explain the photodeprotection reaction.[7a]

Herein, we report for the first time the photorelease of several 1,3-dithiane carbonyl protecting groups by photoinduced oxidation using a 2,4,6-triphenylthiapyrylium cation (**5**) as the sensitizer (Scheme 2). The preparative aspect of the reaction was studied, and a complete mechanistic picture of this photoreaction was established using transient absorption spectroscopy. Additionally, we have used quantum chemical calculations (PCM(ACN)-[M06-2X/def2-TZVP]) for exploring all alternative reaction pathways.

Scheme 2. Dithiane Deprotection Using a Thiapyrylium Cation 5 as the Sensitizer

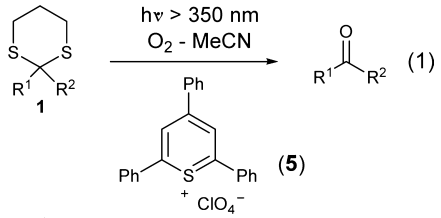

1	a	b	c	d	e
R^1	Ph	4-$OMeC_6H_4$	4-CNC_6H_4	Ph	Ph
R^2	H	H	H	Me	Ph

RESULTS AND DISCUSSION

We studied the reaction between 2-aryl-1,3-dithianes and 2,4,6-triphenylthiapyrylium cation as the sensitizer under both steady-state and time-resolved conditions to assess the photophysical and photochemical behavior of the dithianes and to detect possible transients involved in the photodeprotection process.

Steady-State Photolysis. Photodeprotection of dithianes **1** was conducted in MeCN at $\lambda > 350$ nm using **5** as the sensitizer, and the results are gathered in Table 1. Benzaldehyde was obtained in 42% yield after 2 h irradiation of 2-phenyl-1,3-dithiane (**1a**) in an air-saturated solvent, whereas the reactant conversion was <5% under a nitrogen atmosphere (Table 1, entries 1 and 2). Molecular oxygen is thus essential for the photodeprotection process. Photodeprotection of **1a** was also carried out in a sealed tube, and after a 2 h irradiation, the

Table 1. Photodeprotection of Dithiane 1 in the Presence of 5[a]

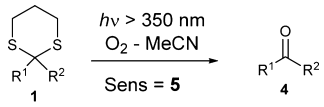

		dithiane **1**		
entry		R^1	R^2	product **4** (%)[b]
1	**1a**	Ph	H	42
2[c]	**1a**	Ph	H	<5
3[d]	**1a**	Ph	H	55[e]
4[f]	**1a**	Ph	H	23
5	**1b**	4-$OMeC_6H_4$	H	27
6	**1c**	4-CNC_6H_4	H	27
7	**1d**	Ph	Me	76
8	**1e**	Ph	Ph	89
9[g]	**1e**	Ph	Ph	85[e,h]

[a]Reaction performed in air-saturated MeCN, [**1**] = 10 mM. [b]Quantification by GC (internal standard method). [c]Under a nitrogen atmosphere. [d]Reaction performed in a sealed tube. [e]Relative areas determined by GC-MS together with a similar amount of 1,2-dithiolane. [f]In the presence of 100% benzoquinone (BQ). [g]In the presence of 0.02% $H_2{}^{18}O$ relative to **1e**. [h]No incorporation of ^{18}O in benzophenone was detected by GC-MS.

product mixture was analyzed by gas chromatography-mass spectrometry (GC-MS). Under these conditions, it was possible to detect 1,2-dithiolane in a similar amount (55%) as benzaldehyde (Table 1, entry 3). Finally, the reaction was partially inhibited by *p*-benzoquinone, a well-established superoxide anion trap (Table 1, entry 4).[11] The lack of reaction under nitrogen atmosphere indicates that oxygen is required to obtain conversion yields. Moreover, inhibition of photodeprotection in the presence of *p*-benzoquinone suggests that the superoxide anion might be the species responsible for the deprotection reaction.

The dethioacetalization process was then explored with other dithianes to evaluate the substitution effect at the phenyl ring as well as at the carbon center. The irradiation time was kept constant (2 h) for all of the dithianes (**1a**–**e**). Table 1 shows that the presence of an electron-donating or -withdrawing group on the phenyl ring leads to lower conversion yields (entries 5 and 6), whereas increasing substitution at the pro-carbonyl carbon improves the yield for ketone formation, namely, acetophenone for **1d** and benzophenone for **1e** (entries 7 and 8). Finally, when photodeprotection of **1e** was performed in the presence of $H_2{}^{18}O$ at a concentration similar to that of the dissolved O_2, no labeled ^{18}O incorporation into the benzophenone product was detected by GC-MS (SIM mode). This result eliminates the participation of water as a nucleophile in the deprotection process.

Characterization of Transient Species by Laser Flash Photolysis (LFP). Using LFP, it was possible to detect the formation of radical cations $\mathbf{1a}$–$\mathbf{d}^{\bullet+}$ (Scheme 3). Laser excitation of the thiapyrylium salt at 355 nm resulted in a broad transient absorption between 460 and 600 nm with a lifetime of 2.5 ± 0.2 μs in MeCN measured at 470 nm (Figure 1a), which was assigned to the known T-T transition of **5** according to previously published spectra.[12] In the presence of dithiane **1a**, the kinetic trace at 470 nm decays faster, and pseudo-first-order treatment at low concentration of **1a** led to the determination of the quenching rate constant k_q (Figure

DOI: 10.1021/jo502953t
J. Org. Chem. 2015, 80, 2733–2739

Scheme 3. Generation of Radical Cations 1a−e$^{\bullet+}$

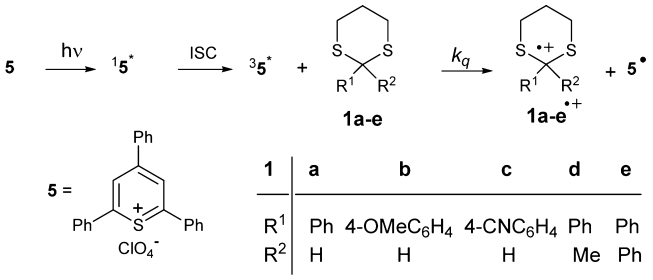

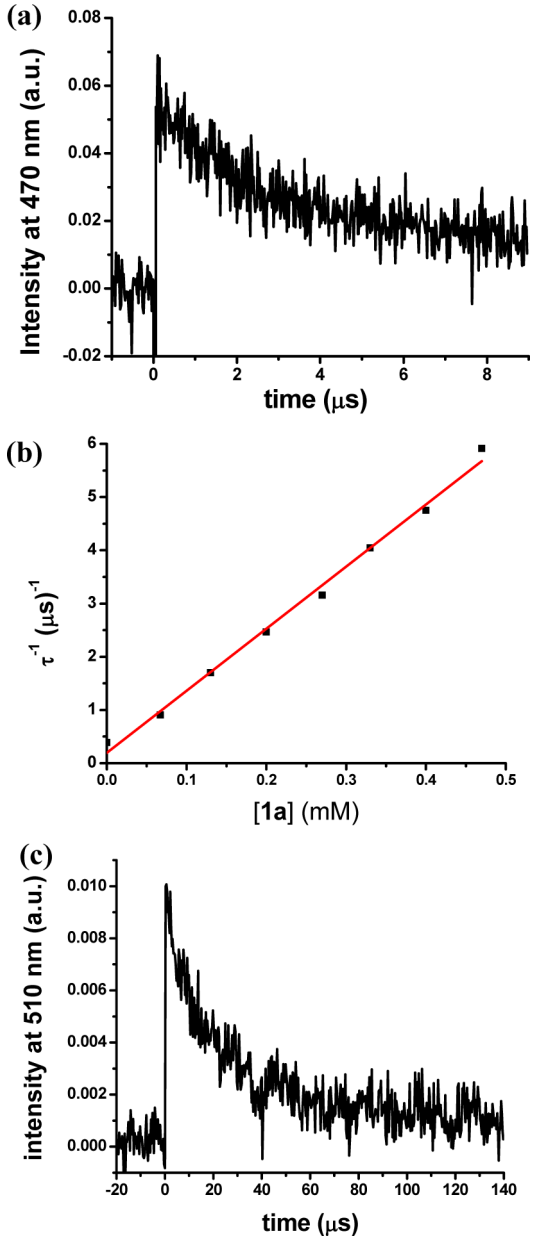

Figure 1. (a) Decay trace of the T-T absorption of **5** (0.067 mM) obtained after laser excitation (λ = 355 nm) in MeCN under argon measured at 470 nm and (b) plot of $1/\tau$ against the concentration of **1a**. (c) Decay trace at 510 nm of a mixture of **5** (0.067 mM) and **1a** (5 mM) obtained after laser excitation (λ = 355 nm) in MeCN under argon.

1b). Concomitant with the disappearance of the triplet **5**, a broad band with a maximum close to 510 nm arises with a longer lifetime of ∼20 μs (Figures 1c and 2) at a relatively high

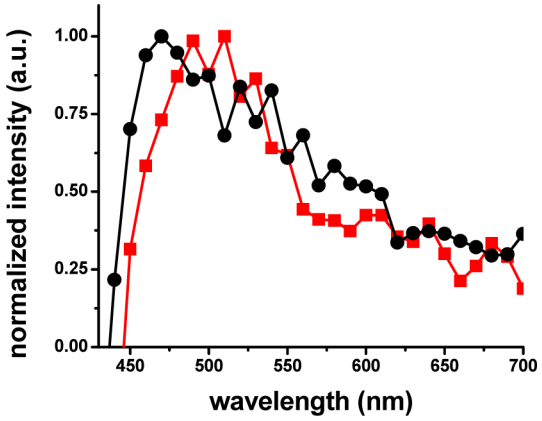

Figure 2. Normalized transient absorption spectra obtained upon LFP (λ = 355 nm) of **5** (0.067 mM) in MeCN under argon with no quencher (●) and with 1 mM of **1a** (red ■) with spectra recorded 0.6 μs after the laser pulse.

concentration of phenyldithiane (5 mM), which was assigned to the 1,3-dithiane radical cation **1a**$^{\bullet+}$. The same methodology was applied to the family of dithianes (**1a−e**). In all of the cases, the triplet state lifetime of the sensitizer in MeCN becomes shorter when increasing the concentration of **1a−e**, and the bimolecular quenching rate constants by these species is in the range of (1.2−2.4) × 10^{10} M^{-1} s^{-1} (Table 2). These

Table 2. Quenching Rate Constants between the Triplet State of 5 and 1a−e and Characteristics of the Dithiane Radical Cations[a]

entry	dithiane	k_q (10^{10} M^{-1} s^{-1})[b]	$\lambda_{max,rad,cat}$ (nm)[c]	$\tau_{rad,cat}$ (μs)[d]	k_Z/k_H[e]
1	1,3-dithiane	1.29	530	30.0	
2	**1a**	1.20	510	20.9	1
3	**1b**	1.40	520	16.0	1.31
4	**1c**	2.37	510	17.2	1.22
5	**1d**	1.35	500	16.7	1.25
6	**1e**	1.38	500	25.1	0.83

[a]In MeCN under argon atmosphere, [**5**] = 0.076 mM; λ_{exc} = 355 nm. [b]Obtained using the Stern−Volmer equation $1/\tau = 1/\tau_0 + k_q[Q]$ at 470 nm. [c]Radical cation wavelength maximum absorption obtained for dithianes **1a−e** (5 mM concentration). [d]Lifetime for radical cations **1a−e**$^{\bullet+}$, assuming a first-order decay. [e]Normalized lifetime of the radical cation toward **1a**$^{\bullet+}$ (effect of the para substituent on the phenyl ring).

quenching rates were ascribed to the electron transfer process from dithianes to the sensitizer triplet state. The Gibbs free energy change for electron transfer (ΔG_{ET}) from dithiane **1b** to the triplet excited state of **5** was estimated according to the Rehm−Weller equation (eq 1),[13] where $E_{D/D^{\bullet+}}$ (the standard oxidation potential of the dithiane) and $E_{A^\bullet/A^-}$ (the standard oxidation potential of the thiapyranyl radical) were obtained from the literature.[14,15] A value of 52 kcal mol^{-1} was used for the excitation energy (E^*), leading to −23 kcal mol^{-1} for ΔG_{ET}, thus indicating that the ET is exergonic. This large driving force is also in agreement with the close to diffusion-controlled

DOI: 10.1021/jo502953t
J. Org. Chem. 2015, 80, 2733−2739

quenching rate constants measured for the investigated dithianes (Table 2).

$$\Delta G_{ET} = 23.06[E_{D/D^{\bullet+}} - E_{A^{\bullet}/A^{+}}] - E_A^* \quad (1)$$

The maximum absorption wavelengths for dithiane radical cations **1a**–**e**$^{\bullet+}$ as well as quenching rate constants for the electron transfer reactions between dithianes **1a**–**e** and the triplet sensitizer are given in Table 2 (kinetic traces are shown in Figures S1–S5 of the Supporting Information).

Fragmentation of the radical cation intermediates could be a unimolecular or bimolecular process assisted by a nucleophilic species. It appears that the decay of the dithiane radical cation signal in all cases follows first-order kinetic behavior and was not affected by the presence of either water or molecular oxygen (e.g., Figure S6 in the Supporting Information), thus confirming the occurrence of a unimolecular decay mechanism in which the nucleophile does not partake. Similar decays profiles were obtained for dithianes bearing electron-releasing and -withdrawing substituents on the aryl moiety (Figures S7 and S8–S12, Supporting Information, for the k_q measurements). Lifetimes for the radical cations **1a**–**e**$^{\bullet+}$, whose values are in the range 16–30 μs, are listed in Table 2.

The dithiane radical cations are stabilized by forming a sulfur–sulfur two-center three-electron bond (i.e., σ type), as already reported for the radical cations of aliphatic sulfides.[16] As a consequence, we expect a small, if any, effect of the substituent on the phenyl ring in dithianes **1a**–**e**. Indeed, the ratio k_Z/k_H shows very little variation across the whole family of compounds (Table 2), thus providing further evidence that C–S bond cleavage occurs without the assistance of a nucleophilic reagent to form a distonic radical cation (Scheme 1), as detailed below.

Mechanism and Theoretical Calculations. Compound **5** is a well-known electron transfer sensitizer with a high singlet excited-state energy (66 kcal mol^{-1}), a triplet excited-state energy of ~52 kcal mol^{-1}, an intersystem crossing quantum yield (Φ_{ISC}) of 0.94, and a reduction potential of −0.21 V relative to the saturated calomel electrode (SCE).[15] In addition, the thiapyrylium salt used does not sensitize the formation of singlet oxygen ($^1\Delta_g$).[17] Our experimental results are consistent with an electron transfer reaction leading to the formation of a dithiane radical cation that further decays to a distonic radical cation. Two species may be formed: an open-benzyl cation (**2**) or a closed-benzyl radical (**3**) (Scheme 1).[7,18] The fact that the decay rates for the radical cations do not depend on the nature of the substituents borne by the dithianes suggests that **3** predominates over **2**. We have performed DFT calculations for **2a** and **3a**, both being derived from C–S bond cleavage in **1a**$^{\bullet+}$ (Scheme 1). In agreement with the experimental data (Table 2), the computational results (Table 3, entries 1 and 2) indicate that **3a** is the most stable structure (by ~9.3 kcal mol^{-1}). In addition, the transition state Gibbs free energy connecting these two structures equals 8.3 kcal mol^{-1} with respect to the open species. The high energy difference between the two structures points toward a strong predominance for the closed form (Figure 3).

It is worth noting that the spin density gives some hints as to the reactivity of each species (Figure 4). In the open form, the spin density on the radical cation is fully located on the external sulfur atom, whereas in the closed form, it is partially delocalized between the benzylic carbon atom and the phenyl ring.

Table 3. Relative Electronic Energy (Zero Point Energy (ZPE) Corrected) and Gibbs Free Energies for Reactions Involving 2a and 3a[a]

entry	reaction	ΔE + ZPE[b] (kcal mol^{-1})	ΔG[b] (kcal mol^{-1})
1	**2a** → **3a**	−9.7	−9.3
2	**2a** →**TS(2a-3a)**	+0.6	+8.3
3	**2a** + H_2O → **TS(H_2O)**	+1.1/+3.4	+16.6/+18.8
4	**2a** + H_2O → **INT(H_2O)**	−18.9/+2.3	−3.3/+18.0
5	**3a** + O_2 ($^3\Sigma_g$) → **TS(O_2)**	+7.1/+5.5	+18.3/+16.6
6	**3a** + O_2 ($^3\Sigma_g$) → **INT(O_2)**	−14.4/−13.0	−2.5/−1.9
7[c]	**3a** + $O_2^{\bullet-}$ → **TS($O_2^{\bullet-}$)**	−13.8	−2.7
8[c]	**3a** + $O_2^{\bullet-}$ → **P**	−64.1	−52.8

[a]Values were computed at the PCM(ACN)-[M06-2X/def2-TZVP] level of theory. [b]Values for entries 3–6 correspond to attack of the nucleophilic species from the internal face (left) and from the external face (right) relative to the dithiane (see Figure 5, path A and B, respectively). [c]Using path A, attack of superoxide anion on **3a** (see Figure 6 and Scheme 3).

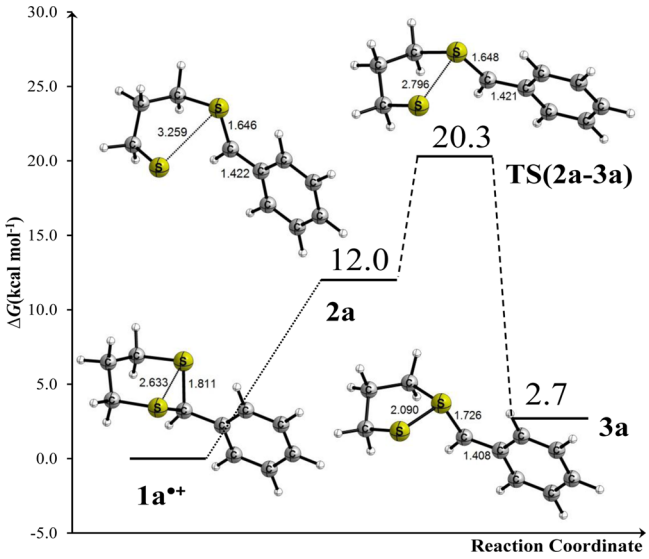

Figure 3. Free energy profile for the closed/open form equilibrium resulting from C–S bond cleavage in the one electron oxidized compound **1a**$^{\bullet+}$. Relative Gibbs free energies are given in kcal mol^{-1}. Selected distances are given in Å.

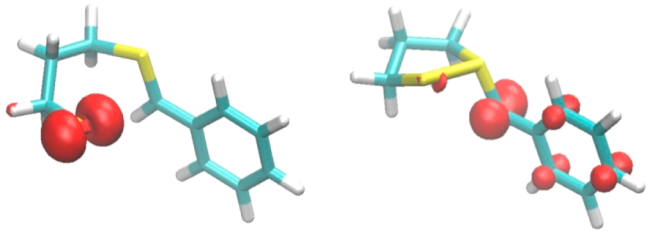

Figure 4. Spin density isosurface (isocontour 0.01 au) for **2a** (left) and **3a** (right). Light blue, carbon; white, hydrogen; and gold, sulfur.

As illustrated in Scheme 1, different nucleophilic species may be responsible for the deprotection reaction, namely, water, molecular oxygen O_2 ($^3\Sigma_g$), and the superoxide anion $O_2^{\bullet-}$. It is commonly accepted that following the formation of the radical cation intermediate, a nucleophilic attack occurs at the benzylic carbon.[7] Taking into account the spin density profiles of **2a** and **3a** as depicted in Figure 4, it can be foreseen that H_2O would

DOI: 10.1021/jo502953t
J. Org. Chem. 2015, 80, 2733–2739

more likely react with the distonic radical cation **2a** at the benzylic carbocation, whereas O_2 ($^3\Sigma_g$) would rather react with **3a** at the benzylic radical. The superoxide anion $O_2^{\bullet-}$ may react as both a nucleophile and radical. We thus performed a computational study of the reaction between the nucleophilic agents and 2-phenyl-1,3-dithiane radical cations in MeCN as the solvent. All of the reaction pathways were calculated at the PCM(ACN)-[M06-2X/def2-TZVP] level of theory.

We first addressed the reaction with water. It has repeatedly been suggested that the presence of water is necessary for getting mild and efficient photochemical and thermal thioacetal deprotection reactions to proceed.[7c,19] The nucleophilic addition of H_2O at the positively charged benzylic carbon of **2a** may occur on two distinct faces. Our results indicate that it takes place on the internal face close to both sulfur atoms (Figure 5, path A) and that the reaction goes through an early

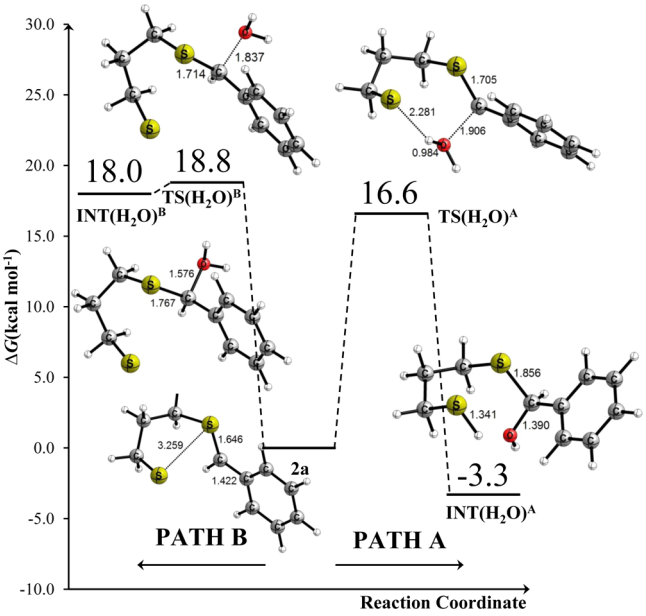

Figure 5. Energy profile for the reaction of the opened 1,2-dithiolane distonic radical cation (**2a**) with water. Relative Gibbs free energies given in kcal mol^{-1}.

transition state where the hydrogen transfer from the water to the sulfur is concerted with the formation of the O−C bond. Such transition states have been observed in reactions involving water molecule and radical species.[20] On the other hand, when the water molecule attacks on the external side, the transition state eigenvector is characterized by the O−C bond formation only (Figure 5, path B).

Both relative electronic energy and Gibbs free energy for the TS are given in entry 3 of Table 3. Path A (Figure 5) is favored both kinetically and thermodynamically. The adduct formed along path B is only 0.8 kcal mol^{-1} below the energy of the corresponding transition state such that if addition of water was to take place along this route, the adduct would immediately evolve back into the reactants.

O_2 ($^3\Sigma_g$) is also an efficient reactant for oxidation processes similar to the well-known free radical oxidation of unsaturated lipids or aldehyde formation by α deprotonation of sulfide radical cations followed by oxygen addition to the carbon-centered radical.[21] It can be seen that the energy of the reaction **3a** + O_2 ($^3\Sigma_g$) → **INT(O$_2$)** is slightly exergonic by 2.5 or 1.9 kcal mol^{-1} depending on the approach (Table 3). However, the calculated energy barriers are high (i.e., 18.3 and 16.6 kcal mol^{-1} for each reactive face).

Finally, it has been suggested that the reaction of the sulfide radical cation with $O_2^{\bullet-}$ may also play a key role in the product formation of different sulfide compounds.[22] On the basis of previous studies on radical cation sulfide derivatives, there are at least five main possible reactions between the dithiane radical cation and $O_2^{\bullet-}$, as illustrated in Scheme 4. The first reaction

Scheme 4. Possible Reactions of 2a and 3a with Superoxide Anion $O_2^{\bullet-}$ through (A) Direct Nucleophilic Addition, (B) Attack on the Internal Sulfur Atom, (C) Attack on the External Sulfur Atom, (D) Back Electron Transfer, and (E) Deprotonation

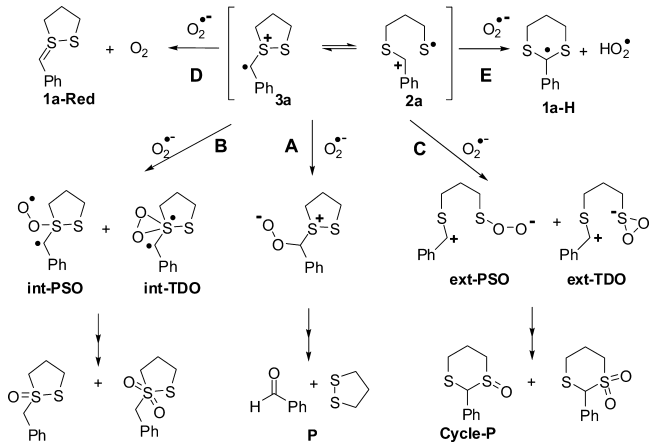

(path A) is nucleophilic addition to the carbon atom bearing a partial positive charge. The second reaction (path B) consists of an $O_2^{\bullet-}$ attack on the internal sulfur atom to yield persulfoxide (**int-PSO**) and/or thiadioxirane (**int-TDO**), as reported elsewhere.[22a] Likewise, the attack can occur at the external sulfur atom to give persulfenate (**ext-PST**) and/or thiadioxirane (**ext-TDO**)[23] along path C. Addition of $O_2^{\bullet-}$ to the sulfide radical cation has been demonstrated to take place for other systems,[22b,24] but its efficiency depends on side reactions such as back electron transfer (path D) and deprotonation (path E). Deprotonation following oxidation is a common reaction mechanism for benzyl sulfide derivates, and it has been shown to be thermodynamically favored for some systems.[25] In the present case, abstraction of the benzylic proton by radical anion superoxide (path E) is thermodynamically unfavorable because ΔH^0 and ΔG^0 are 11.9 and 10.5 kcal mol^{-1}, respectively. On the other hand, back electron transfer is highly exergonic, ΔG^0 = −37.9 kcal mol^{-1} (path D), and might affect the yield of the photooxidation reaction.

We have explored the various paths displayed in Scheme 4. Relative energies of the structures with respect to reactants are displayed in Figure S13 in the Supporting Information. The Gibbs free energy of product **P** (Scheme 4, path A), formed by direct attack of the $O_2^{\bullet-}$ on the electrophilic carbon, stands 52.8 kcal mol^{-1} below the energy of the reactants. This value is in line with a barrierless attachment of $O_2^{\bullet-}$. In fact, the energy of the transition state connecting **3a** to **P** is −2.7 kcal mol^{-1} below **3a**, (Table 3, entry 7). The energy profile is presented in Figure 6, where the reaction with H_2O and O_2 ($^3\Sigma_g$) were included in blue and red, respectively, for comparison. From this picture, it appears that the reaction between **3a** and $O_2^{\bullet-}$ is

DOI: 10.1021/jo502953t
J. Org. Chem. 2015, 80, 2733−2739

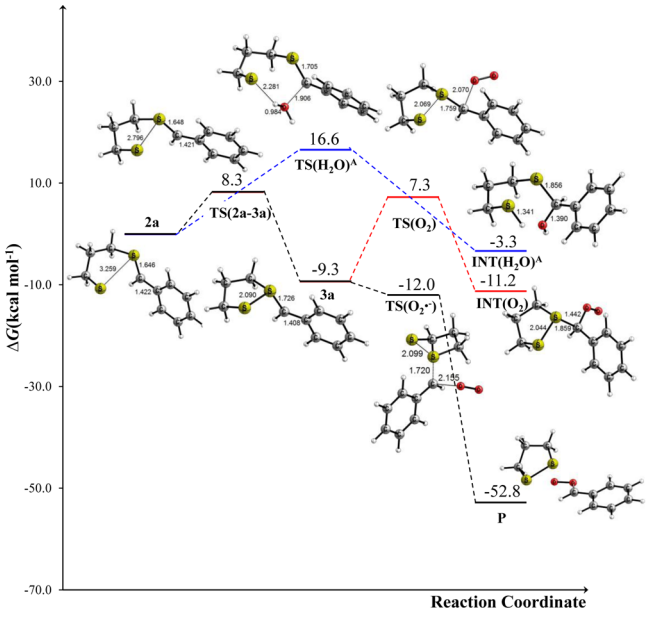

Figure 6. Energy profile for the reaction of **2a** and **3a** with water (blue line), O_2 ($^3\Sigma_g$) (red line), and $O_2^{\bullet-}$ (black line). Relative Gibbs free energies given in kcal mol^{-1}.

the most favorable route for the deprotection process both kinetically and thermodynamically.

Conversely to the addition of water and molecular oxygen, the $O_2^{\bullet-}$ approach through the internal face of **2a** leads to the formation of a persulfenate species (**ext-PST**, path C in Scheme 4), that is 15.1 kcal mol^{-1} more stable than the initial reagents. Cyclisation by reaction at the carbon atom leads to **Cycle-P** (see Figure S13 in the Supporting Information) through a 3 kcal mol^{-1} barrier, whereas the process is exergonic by 6.5 kcal mol^{-1}.

The addition of $O_2^{\bullet-}$ to the internal sulfur of **3a** yields the thiadioxirane compound **int-TDO** (Scheme 4, path B), which is slightly exothermic (ΔH^0 = −8.0 kcal mol^{-1}) but unfavorable in terms of Gibbs free energy (ΔG^0 = 5.8 kcal mol^{-1}, see Figure S13 in the Supporting Information). Similarly, the reaction leading to the persulfoxide adduct (**int-PSO**) is endergonic by 6.3 kcal mol^{-1}. The transition state connecting these two structures was found to be 17.9 kcal mol^{-1} higher in energy with respect to the reactant energy and 12.1 kcal mol^{-1} with respect to **int-TDO** (Figure S13 in the Supporting Information). This is in good agreement with the values reported for the isomerization process with dimethyl sulfide.[26]

CONCLUSIONS

We elucidated the mechanistic details of the photodeprotection reaction of 1,3-dithiane derivates by a combination of experimental and computational studies. Comparative experiments performed under nitrogen atmosphere and in the presence of the $H_2{}^{18}O$ indicate that oxygen plays a crucial role in the reaction. Inhibition of the reaction with *p*-benzoquinone further supports the notion that the superoxide radical anion is the most probable source of oxygen. Using laser flash photolysis experiments, we were able to characterize a dithiane radical cation species as an intermediate during the course of the reaction. The effects of water, molecular oxygen, and the substituents of the aryl group on the decay rate constant of the intermediate all support unimolecular fragmentation.

All of these experimental outcomes can be rationalized by a stepwise mechanism in which a first single electron transfer is followed by unimolecular fragmentation, yielding a distonic radical cation that then reacts quickly with the superoxide anion. This picture is in agreement with theoretical calculations. Exploration of the various reaction routes indeed supports the proposal that the reaction of oxidized dithianes with the superoxide radical anion is the most favorable pathway on both kinetic and thermodynamic grounds.

EXPERIMENTAL SECTION

Materials and Methods. The chemicals acetophenone and benzophenone were purchased. Acetonitrile (HPLC grade) was used without any further purification and stored over molecular sieves (4 Å). Ultrapure water from a Milli-Q station was used. All dithianes and 2,4,6-triphenylthiapyrylium perchlorate were synthesized and purified according to previously reported procedures.[27,28] Absorption measurements were performed with a UV−Visible spectrophotometer. For laser flash photolysis (LFP), transient absorption spectra and quenching rate constants were determined using a Nd:YAG laser generating a 355 nm laser pulse (10 mJ per pulse, ∼10 ns pulse duration) as an excitation source. The spectrometer was a commercial setup.

Computational Details. Theoretical calculations were performed with the GAUSSIAN 09 suite of programs.[29] All geometry optimizations were computed using the functional M06-2X[30] and the Ahlrich def2-TZVP basis set.[31] The stationary points were located with the Berny algorithm[32] using redundant internal coordinates. Analytical Hessians were computed to determine the nature of the stationary points (one and zero imaginary frequencies for transition states and minima, respectively)[33] and to calculate unscaled zero-point energies (ZPEs) as well as thermal corrections and entropic effects using the standard statistical mechanics relationships for an ideal gas.[34] Transition structures (TSs) show only one negative eigenvalue in their diagonalized force constant matrices, and their associated eigenvectors were confirmed to correspond to the motion along the reaction coordinate under consideration using the intrinsic reaction coordinate (IRC) method.[35] Unless otherwise stated, Gibbs energies have been computed at 298.15 K. For these calculations, the acetonitrile solvent was described by nonspecific solvent effects within the self-consistent reaction field (SCRF) approach in Tomasi's formalism.[36]

Representative Experimental Procedure for the Deprotection Process. A solution of dithiane (0.1 mmol, 10 mM) and 2,4,6-triphenylthiapyrylium (1 mM) in acetonitrile was irradiated with a medium pressure Hg lamp in a Pyrex tube while being purged with a stream of oxygen. After irradiation, the products were quantified by GC using the internal standard method.

ASSOCIATED CONTENT

Supporting Information

Transient dithiane spectra, substituent effects, triplet quenching plots, energy profiles, theoretical structures. This material is available free of charge via the Internet at http://pubs.acs.org.

AUTHOR INFORMATION

Corresponding Authors

*E-mail: robert@univ-paris-diderot.fr.

*E-mail: penenory@fcq.unc.edu.ar.

Notes

The authors declare no competing financial interest.

ACKNOWLEDGMENTS

Authors acknowledge ECOS-Sud (Grant A10E03), INFIQC−CONICET, and Universidad Nacional de Córdoba (UNC). This work was partially supported by MINCyT-ECOS, CONICET, SECyT-UNC, and FONCyT. D.M.A. thanks

DOI: 10.1021/jo502953t
J. Org. Chem. 2015, 80, 2733−2739

Deutscher Akademischer Austausch Dienst for a postdoctoral fellowship (Grant A/12/76196).

REFERENCES

(1) (a) Greene, T. W.; Wuts, P. G. M. *Protective Groups in Organic Synthesis*, 3rd ed.; John Wiley & Sons: New York, 1999. (b) Kocienski, P. J. *Protecting Groups*; George Thieme: Stuttgart, Germany, 1994.

(2) (a) Burghardt, T. E. *J. Sulfur Chem.* **2005**, *26*, 411−427. (b) Banerjee, A. K. *Russ. Chem. Rev.* **2000**, *69*, 947−955.

(3) (a) Mahapatra, A. K.; Maji, R.; Sahoo, P.; Nandi, P. K.; Mukhopadhyay, S. K.; Banik, A. *Tetrahedron Lett.* **2012**, *53*, 7031−7035. (b) Mahapatra, A. K.; Roy, J.; Sahoo, P. *Tetrahedron Lett.* **2011**, *52*, 2965−2968.

(4) (a) Hirano, M.; Ukawa, K.; Yakabe, S.; Clark, J. H.; Morimoto, T. *Synthesis* **1997**, 858−860. (b) Kamal, A.; Laxman, E.; Reddy, P. S. M. M. *Synlett* **2000**, 1476−1478.

(5) Lee, J. G.; Hwang, J. P. *Chem. Lett.* **1995**, 507−508.

(6) (a) Gupta, N.; Sonu, G.; Kad, L.; Singh, J. *Catal. Commun.* **2007**, 1323−1328. (b) Oksdath-Mansilla, G.; Peñéñory, A. B. *Tetrahedron Lett.* **2007**, *48*, 6150−6154.

(7) (a) Kamata, M.; Sato, M.; Hasegawa, E. *Tetrahedron Lett.* **1992**, *33*, 5085−5088. (b) Kamata, M.; Kato, M.; Hasegawa, E. *Tetrahedron Lett.* **1991**, *32*, 4349−4352. (c) Kamata, M.; Murakami, Y.; Tamagawa, Y.; Kato, Y.; Hasegawa, E. *Tetrahedron* **1994**, *50*, 12821−12828. (d) Epling, G. A.; Wang, Q. *Tetrahedron Lett.* **1992**, *33*, 5909−5912. (e) Fasani, E.; Freccero, M.; Mella, M.; Albini, A. *Tetrahedron* **1997**, *53*, 2219−2232.

(8) Kamata, M.; Otogawa, H.; Hasegawa, E. *Tetrahedron Lett.* **1991**, *32*, 7421−7424.

(9) Platen, M.; Steckhan, E. *Tetrahedron Lett.* **1980**, *21*, 511−514.

(10) Schmittel, M.; Levis, M. *Synlett* **1996**, 315−316.

(11) Manring, L. E.; Kramer, M. K.; Foote, C. S. *Tetrahedron Lett.* **1984**, *25*, 2523−2526.

(12) Akaba, R.; Kamata, M.; Koike, A.; Mogi, K. I.; Kuriyama, Y.; Sakuragi, H. *J. Phys. Org. Chem.* **1997**, *10*, 861−869.

(13) (a) Weller, A. *Z. Phys. Chem.* **1982**, *133*, 93−98. (b) Rehm, D.; Weller, A. *Isr. J. Chem.* **1970**, *8*, 259−271.

(14) E_p^{ox} (**1b**) = 1.04 V (vs SCE in MeCN), see ref 8.

(15) Triplet energy of thiapyrylium salt (**5**) = 52 kcal mol^{-1}, and a reduction potential of −0.21 V versus SCE has been measured. Miranda, M. A.; García, H. *Chem. Rev.* **1994**, *94*, 1063−1089.

(16) (a) Chaudhri, S. A.; Mohan, H.; Anklam, E.; Asmus, K.-D. *J. Chem. Soc., Perkin Trans. 2* **1996**, 383−390. (b) James, M. A.; McKee, M. L.; Illies, A. J. *J. Am. Chem. Soc.* **1996**, *118*, 7836−7842. (c) Asmus, K.-D. *Acc. Chem. Res.* **1979**, *12*, 436−442.

(17) Miranda, M. A.; Izquierdo, M. A.; Pérez-Ruiz, R. C. *J. Phys. Chem. A* **2003**, *107*, 2478−2482.

(18) (a) Pandey, B.; Bal, S. Y.; Khire, U. R.; Rao, A. T. *J. Chem. Soc., Perkin Trans. 1* **1990**, 3217−3218. (b) Kamata, M.; Nagai, S.; Kato, M.; Hasegawa, E. *Tetrahedron Lett.* **1996**, *37*, 7779−7782. (c) Roth, H. D.; Shen, K.; Lakkaraju, P. S.; Fernández, L. *Chem. Commun. (Cambridge, U.K.)* **1998**, 2447−2448.

(19) (a) Mathew, L.; Sankararaman, S. *J. Org. Chem.* **1993**, *58*, 7576−7577. (b) Tanemura, K.; Dohya, H.; Imamura, M.; Suzuki, T.; Horaguchi, T. *J. Chem. Soc., Perkin Trans. 1* **1996**, 453−457.

(20) Méndez-Hurtado, J.; López, R.; Suárez, D.; Menéndez, M. I. *Chem.—Eur. J.* **2012**, *18*, 8437−8447.

(21) (a) Baciocchi, E.; Crescenzi, C.; Lanzalunga, O. *Tetrahedron* **1997**, *53*, 4469−4478. (b) Yin, H.; Xu, L.; Porter, N. A. *Chem. Rev.* **2011**, *111*, 5944−5972.

(22) (a) Baciocchi, E.; Del Giacco, T.; Elisei, F.; Gerini, M. F.; Guerra, M.; Lapi, A.; Liberali, P. *J. Am. Chem. Soc.* **2003**, *125*, 16444−16454. (b) Baciocchi, E.; Del Giacco, T.; Giombolini, P.; Lanzalunga, O. *Tetrahedron* **2006**, *62*, 6566−6573. (c) Che, Y.; Ma, W.; Ren, Y.; Chen, C.; Zhang, X.; Zhao, J.; Zang, L. *J. Phys. Chem. B* **2005**, *109*, 8270−8276.

(23) Note that the term "thiadioxirane" refers to a compound with the formula R_2SO_2, where a three-membered ring is formed between the S and the two O atoms. Although **ext-TDO** is not strictly a thiadioxirane species, it has the main ring.

(24) (a) Ando, W.; Kabe, Y.; Kobayashi, S.; Takyu, C.; Yamagishi, A.; Inaba, H. *J. Am. Chem. Soc.* **1980**, *102*, 4526−4528. (b) Clennan, E. L. *Acc. Chem. Res.* **2001**, *34*, 875−884. (c) Miller, B. L.; Williams, T. D.; Schöneich, C. T. *J. Am. Chem. Soc.* **1996**, *118*, 11014−11025.

(25) (a) Freccero, M.; Pratt, A.; Albini, A.; Long, C. *J. Am. Chem. Soc.* **1998**, *120*, 284−297. (b) Baciocchi, E.; Bietti, M.; Lanzalunga, O. *J. Phys. Org. Chem.* **2006**, *19*, 467−478.

(26) Jensen, F.; Greer, A.; Clennan, E. L. *J. Am. Chem. Soc.* **1998**, *120*, 4439−4449.

(27) Firouzabadi, H.; Iranpoor, N.; Hazarkhani, H. *J. Org. Chem.* **2001**, *66*, 7527−7529.

(28) Wizinger, R.; Ulrich, P. *Helv. Chim. Acta* **1956**, *39*, 1−4.

(29) Frisch, M. J.; Trucks, G. W.; Schlegel, H. B.; Scuseria, G. E.; Robb, M. A.; Cheeseman, J. R.; Scalmani, G.; Barone, V.; Mennucci, B.; Petersson, G. A.; Nakatsuji, H.; Caricato, M.; Li, X.; Hratchian, H. P.; Izmaylov, A. F.; Bloino, J.; Zheng, G.; Sonnenberg, J. L.; Hada, M.; Ehara, M.; Toyota, K.; Fukuda, R.; Hasegawa, J.; Ishida, M.; Nakajima, T.; Honda, Y.; Kitao, O.; Nakai, H.; Vreven, T.; Montgomery, J. A., Jr.; Peralta, J. E.; Ogliaro, F.; Bearpark, M.; Heyd, J. J.; Brothers, E.; Kudin, K. N.; Staroverov, V. N.; Kobayashi, R.; Normand, J.; Raghavachari, K.; Rendell, A.; Burant, J. C.; Iyengar, S. S.; Tomasi, J.; Cossi, M.; Rega, N.; Millam, J. M.; Klene, M.; Knox, J. E.; Cross, M. J. B.; Bakken, V.; Adamo, C.; Jaramillo, J.; Gomperts, R.; Stratmann, R. E.; Yazyev, O.; Austin, A. J.; Cammi, R.; Pomelli, C.; Ochterski, J. W.; Martin, R. L.; Morokuma, K.; Zakrzewski, V. G.; Voth, G. A.; Salvador, P.; Dannenberg, J. J.; Dapprich, S.; Daniels, A. D.; Farkas, O.; Foresman, J. B.; Ortiz, J. V.; Cioslowski, J.; Fox, D. J. *Gaussian 09*, revision C.01; Gaussian, Inc.: Wallingford, CT, 2009.

(30) Zhao, Y.; Truhlar, D. G. *Theor. Chem. Acc.* **2008**, *120*, 215−241.

(31) Weigend, F.; Ahlrichs, R. *Phys. Chem. Chem. Phys.* **2005**, *7*, 3297−3305.

(32) Peng, C. Y.; Ayala, P. Y.; Schlegel, H. B.; Frisch, M. J. *J. Comput. Chem.* **1996**, *17*, 49−56.

(33) McIver, J. W.; Komornic, A. *J. Am. Chem. Soc.* **1972**, *94*, 2625−2633.

(34) Atkins, P. W.; De Paula, J. *Physical Chemistry*, 8th ed.; Oxford: Oxford University Press: Oxford, U.K., 2006.

(35) González, C.; Schlegel, H. B. *J. Phys. Chem.* **1990**, *94*, 5523−5527.

(36) (a) Miertus, S.; Scrocco, E.; Tomasi, J. *Chem. Phys.* **1981**, *55*, 117−129. (b) Barone, V.; Cossi, M.; Tomasi, J. *J. Comput. Chem.* **1998**, *19*, 404−417.

DOI: 10.1021/jo502953t
J. Org. Chem. 2015, 80, 2733−2739